Bioinorganic Chemistry

Spin-State Rationale for the Peroxo-Stabilizing Role of the Thiolate Ligand in Superoxide Reductase**

Michael R. Bukowski, Heather L. Halfen, Tieme A. van den Berg, Jason A. Halfen, and Lawrence Que, Jr.**

Nature uses cysteine to modulate the electronic properties of the metal centers in metalloproteins.[1] Particularly interesting is the contrast in function between two mononuclear iron enzymes with similar square pyramidal $\{Fe^{II}(N)_4(Cys_{apical})\}$ active sites: cytochrome P450[2] and superoxide reductase (SOR).[3,4] The well-studied cytochrome P450 has an $\{Fe^{II}$-(porphyrin dianion)(Cys)$\}$ site that activates dioxygen to oxidize hydrocarbon substrates.[5] Dioxygen activation is proposed to occur via a low-spin Fe^{III}-OOH intermediate that converts into a high-valent iron-oxo oxidizing species[6,7] with the heterolytic O–O bond-cleavage step assisted by a "push" of electron density from the *trans* thiolate ligand (Scheme 1 A).[8] In contrast, superoxide reductase (SOR) uses a similar $\{Fe^{II}(His)_4(Cys)\}$ site to convert superoxide into hydrogen peroxide as a means of protecting anaerobes and microaerophiles from the inimical effects of superoxide that may be formed from occasional intrusion of O_2 into the cell.[9] The superoxide reduction mechanism is proposed to go through an iron(III)-peroxo intermediate that undergoes protonation at both oxygen centers to release H_2O_2 (Scheme 1 B).[10–12] It has been suggested that the difference in function between P450 and SOR arises from the different spin states of the intermediates.[9,11,13] To understand nature's rationale for using such similar active sites for apparently opposite functions, we have carried out a systematic study of a series of square pyramidal $[Fe^{II}(L^8py_2)(X_{apical})]$ precursor complexes, where L^8py_2 is a tetradentate nonheme ligand *N*,*N*′-bis(2-pyridylmethyl)-1,5-diazacyclooctane that is constrained to adopt a near planar arrangement of four nitrogen atoms[14] and X_{apical} can be triflate (**1**), benzoate (**2**), or 4-methylbenzenethiolate (**3**; Scheme 2). These complexes react with *t*BuOOH to afford high-spin alkylperoxoiron(III) intermediates. We find that the more basic apical ligand enhances

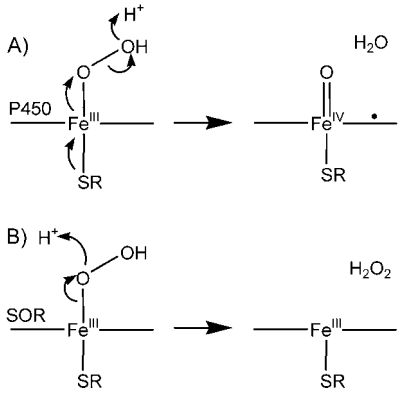

Scheme 1.

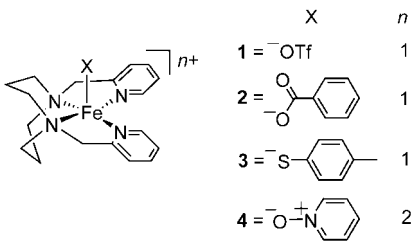

Scheme 2.

[*] M. R. Bukowski, T. A. van den Berg, Prof. Dr. L. Que, Jr.
Center for Metals in Biocatalysis and
Department of Chemistry
University of Minnesota
207 Pleasant Street SE, Minneapolis, MN 55455 (USA)
Fax: (+1) 612-624-7029
E-mail: que@chem.umn.edu
H. L. Halfen, Prof. Dr. J. A. Halfen
Deparment of Chemistry
University of Wisconsin-Eau Claire
105 Garfield Avenue, Eau Claire, WI 54702 (USA)
Fax: (+1) 715-836-4979
E-mail: halfenja@uwec.edu

[**] This work was supported by grants from the National Science Foundation (CHE-0234951 to J.A.H.) and the National Institutes of Health (GM-33162 to L.Q.). J.A.H. acknowledges sabbatical support from the University of Minnesota NSF/RSEC program (CHE-0113894) and the University of Wisconsin-Eau Claire. The authors would like to acknowledge Dr. Neil R. Brooks, Dr. Victor G. Young, Jr., and the X-Ray Crystallographic Laboratory, Department of Chemistry, University of Minnesota.

  DOI: 10.1002/ange.200461527

the stability of the high-spin Fe^{III}-OOR intermediate, an effect opposite to that deduced for corresponding low-spin centers,[15] which provides a rationale for the presence of an apical thiolate in SOR.

Complexes **1**–**3** (Scheme 2) can be readily obtained in high yield by combining the components in the appropriate solvent. The crystal structures of **1** and **2** shown in Figure 1

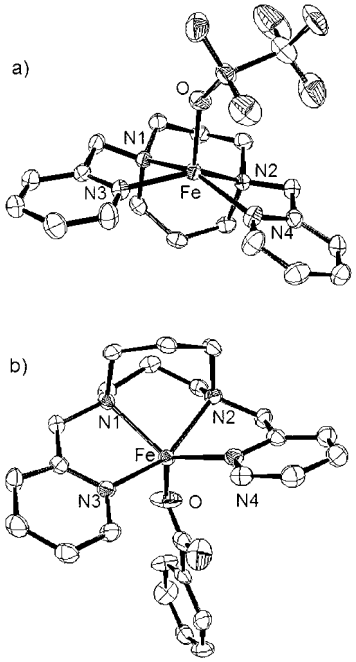

Figure 1. ORTEP plots for a) $[(L^8py_2)Fe(OTf)]^+$ (**1**) and b) $[(L^8py_2)Fe(O_2CPh)]^+$ (**2**) with thermal ellipsoids set at 50% probability. Selected interatomic distances [Å] and angles [°]: a) Fe-N1 2.176(3), Fe-N2 2.216(2), Fe-N3 2.164(3), Fe-N4 2.137(3), Fe-O 2.011(2); N3-Fe-N2 148.60(10), N4-Fe-N1 149.49(11). b) Fe-N1 2.198(3), Fe-N2 2.208(3), Fe-N3 2.164(3), Fe-N4 2.106(3), Fe-O 1.999(3); N3-Fe-N2 129.43(12), N4-Fe-N1 152.60(12).

reveal square pyramidal ($\tau = 0.02$ (**1**) and 0.38 (**2**)) iron(II) centers with the L^8py_2 nitrogen atoms occupying the basal plane and an anionic ligand in the apical site, similar to that reported for **3**.[14] The average Fe–N separation ranges from 2.17 and 2.21 Å, typical of high-spin Fe^{II} complexes with neutral nitrogen-ligand sets[16] and increases in the order of **1**, **2**, **3** in response to the basicity of the apical ligand. In UV/Vis spectra obtained in CH_2Cl_2 solution, **1**–**3** exhibit absorption shoulders at 350, 380, and 400 nm ($\varepsilon \approx$ 500–600 $M^{-1}cm^{-1}$), respectively; the progressive red shift observed correlates with the increased basicity of the apical ligand, so the features can be assigned to iron(II)-to-pyridine charge-transfer transitions.

The reaction of **1** with excess *t*BuOOH in CH_2Cl_2 at −80 °C affords a deep purple chromophore, **1a**, with λ_{max} at 580 nm ($\varepsilon =$ 2500 $M^{-1}cm^{-1}$; Figure 2 and Table 1), parameters comparable to those associated with

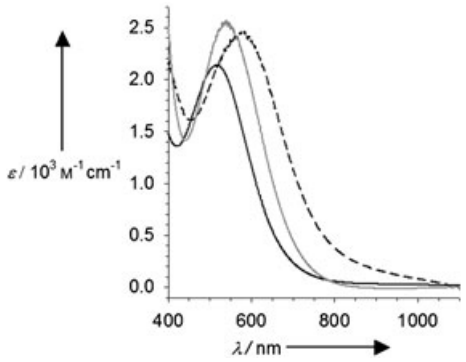

Figure 2. Intermediates **1a** (– – –), **2a** (——), and **3a** (——) generated at −80 °C in CH_2Cl_2.

the reported alkylperoxoiron(III) intermediates.[16–18] Species **1a** exhibits an EPR spectrum with signals at $g = 8.8$, 5.2, and 3.2 that correspond to a high-spin iron(III) ($S = 5/2$) center with $E/D = 0.17$ and a resonance Raman spectrum with four resonance-enhanced vibrations at 463, 627, 833, and 870 cm^{-1} that arise from coordinated alkylperoxide (Figure 3 and Table 1).This pattern of Raman vibrations has been observed for high-spin alkylperoxoiron(III) intermediates and is distinct from that associated with their low-spin counterparts.[16] Thus **1a** can be characterized as the high-spin $[Fe^{III}(L^8py_2)(OO\textit{t}\text{-Bu})(OTf)]^+$ ion.

Parallel reactions using either **2** or **3** yield intermediates **2a** or **3a**, respectively, with absorbance maxima that are blue-shifted relative to that of **1a** (Figure 2, Table 1). The progressive blue shift observed from **1a** to **2a** to **3a** can be rationalized by the substitution of the axial triflate ligand in **1a** with more Lewis basic benzoate and thiolate ligands in **2a** and **3a**, respectively, and confirms the assignment of the chromophore as an alkylperoxo-to-iron(III) charge-transfer transition. Like **1a**, compounds **2a** and **3a** exhibit $S = 5/2$ EPR signals and the same pattern of Raman vibrations (Table 1; Figure 3). These three species thus constitute a series of high-spin Fe^{III}-OO*t*Bu intermediates.

Intermediates **1a**–**3a** are stable for hours at −80 °C but exhibit differing lifetimes at −40 °C. Intermediate **1a** formed with 3 equivalents *t*BuOOH at −40 °C decays completely

Table 1: Properties of $[Fe^{III}(L)(OO\textit{t}Bu)(X)]$ Intermediates.

	Solvent	Spin-State (E/D)	λ_{max} [nm]	ε [$M^{-1}cm^{-1}$]	δ_{tBu} [cm^{-1}]	ν_{Fe-O} [cm^{-1}]	ν_{O-O} [cm^{-1}]	k_{dec}[a] [s^{-1}]
$L = L^8py_2$								
1a (X = OTf)	CH_2Cl_2	5/2 (0.17)	580	2500	463	627	833, 870	1.8×10^{-2}
2a (X = OBz)	CH_2Cl_2	5/2 (0.17)	545	2700	463	623	832, 873	5.4×10^{-4}
3a (X = SAr)	CH_2Cl_2	5/2 (0.20)	510	2200	461	623	830, 874	5.8×10^{-5}
4a (X = pyO)	CH_2Cl_2	5/2 (0.18)	550	2450	463	623	831, 878	8.2×10^{-4}
6-Me_3-TPA[b]	CH_3CN	5/2 (0.33)	562	2200	468	637	842, 877	
TPA[b]	CH_3CN	1/2	600	2000	490	696	796	

[a] 1 mM Fe, 3 equiv *t*BuOOH, −40 °C in CH_2Cl_2. [b] From Ref. [16].

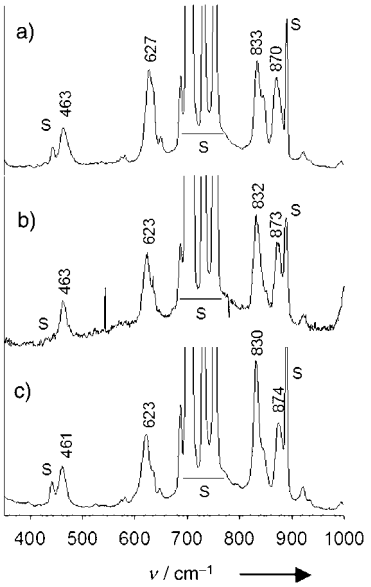

Figure 3. Resonance Raman spectra of a) **1a**, b) **2a**, and c) **3a** in CH_2Cl_2 at 77 K (λ_{ex} = 514.5 nm, power = 100 mW).

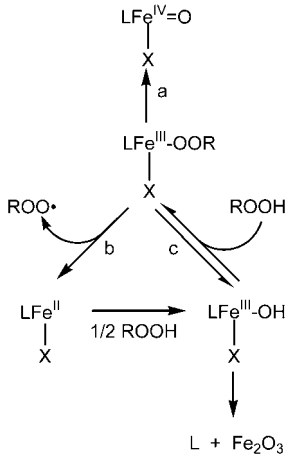

Scheme 3.

within 7 minutes in a first order process ($k = 1.8(1) \times 10^{-2}\ s^{-1}$). In contrast, **2a** and **3a** formed under these conditions are more stable by approximately two orders of magnitude, requiring 5 and 14 h, respectively, for complete decay. Thus a more basic axial ligand appears to stabilize the Fe^{III}-OO*t*Bu unit.

The stabilizing effect of a Lewis basic sixth ligand observed for the $[Fe^{III}(L^8py_2)(OOtBu)(X)]^{n+}$ series is opposite to that recently demonstrated for the mononuclear $[Fe^{III}$-(TPA)(OO*t*Bu)] complex (TPA = tris(2-pyridylmethyl)amine).[15] In the $[Fe^{III}(TPA)(OOtBu)]^{2+}$ complex, decomposition of the TPA intermediate to form $[Fe^{IV}(O)(TPA)]^{2+}$ at −40 °C is greatly accelerated by pyridine N-oxide (PyO). In contrast, the addition of PyO to **1a** significantly retards its decay ($k = 8.2 \times 10^{-4}\ s^{-1}$) and results in a blue shift in the alkylperoxo-to-iron(III) charge-transfer band (λ_{max} = 550 nm). This new species, designated **4a**, is characterized as a high-spin Fe^{III}-OO*t*Bu intermediate with PyO as the sixth ligand on the basis of the similarity of its UV/Vis, EPR, and resonance Raman spectroscopic features to those of **1a**–**3a** (Table 1). The effect of PyO on the λ_{max} and the stability of the Fe^{III}-OO*t*Bu unit is consistent with its expected Lewis basicity, which lies between those of triflate and benzoate.

The stabilizing effect of Lewis bases observed for the L^8py_2 series of iron peroxo complexes clearly contrasts the destabilizing effect observed for $[Fe^{III}(TPA)(OOR)]^{2+}$ intermediates[15,19] and the "push" effect that promotes O–O bond cleavage in heme systems.[5] We attribute these opposing effects to the difference in the spin states of the peroxoiron(III) species: high spin for the L^8py_2 series and low spin for TPA and heme complexes. Earlier Raman studies of end-on bound hydroperoxo- and alkylperoxoiron(III) species have shown that low-spin centers give rise to stronger Fe–O and weaker O–O bonds, thereby setting the stage for O–O bond cleavage (Scheme 3, pathway a); electron donation to the metal center would then facilitate access to the iron(IV) oxidation state.[18,20,21] High-spin centers, on the other hand, give rise to the opposite effect, affording weaker Fe–O and stronger O–O bonds that favor Fe–O bond homolysis instead as a decomposition pathway for the peroxoiron(III) species to form iron(II) and peroxyl radicals (Scheme 3, pathway b).[17] In this case, electron donation to the metal center would lower the $Fe^{III/II}$ potential and be expected to retard the decay. This outcome has been observed for a series of high-spin $[Fe^{III}(6$-Me_3-TPA)(OO*t*Bu)$(O_2CC_6H_4$-X)$]^+$ complexes, where decay by Fe–O bond homolysis is promoted by electron-withdrawing substituents and the lifetime of the intermediate is prolonged by electron-donating groups.[22] The L^8py_2 series reported herein further illustrates this notion by expanding the range of sixth ligands and including the thiolate relevant to SOR chemistry. Indeed the thiolate ligand provides the longest lived peroxoiron(III) species in the L^8py_2 series.

Intermediates **1a**–**3a** decay to yield an Fe_2O_3 precipitate and free ligand. We speculate that these products are obtained because of the instability of the $[Fe^{III}(L^8py_2)OH]^{2+}$ intermediate proposed in Scheme 3, which is consistent with the fact that we have been unable to obtain $\{Fe^{III}(L^8py_2)\}$ complexes by direct synthesis from iron(III) salts. The putative $[Fe^{III}(L^8py_2)OH]^{2+}$ intermediate may be formed in two steps by pathway b in Scheme 3 and subsequent oxidation of the resulting iron(II) precursor by residual *t*BuOOH or in one step by hydrolysis (pathway c). Indeed pathway c may be expected to become more important with a more electron-donating sixth ligand.

The current data allow us to speculate on the function of the high-spin $\{Fe(His)_4(Cys)\}$ active site of SOR. The electron-rich thiolate would be expected to lower the $Fe^{III/II}$ potential and promote the reduction of superoxide to form a high-spin peroxoiron(III) intermediate. The O–O bond cleavage to produce undesired high-valent oxoiron species is prevented by the high-spin iron(III) center and the presence of the axial thiolate ligand. These features may also function to prolong the lifetime of the peroxoiron(III) species to allow its protonation by a second-sphere residue and subsequent

release of H_2O_2. The contrasting effects of Lewis bases on the stability of low-spin and high-spin peroxoiron(III) species thus provide a rationale for nature's use of an axial thiolate in cytochrome P450 and SOR for two apparently distinct roles.

Experimental Section

1: Solutions of L^8py_2 (68.0 mg, 0.229 mmol) in anhydrous, inhibitor-free THF (5 mL) and $[Fe(MeCN)_2(OTf)_2]$ (105 mg, 0.240 mmol) in a minimum of acetonitrile were combined and stirred for 20 min at ambient temperature then left to stand at −30 °C. Large, colorless crystals suitable for X-ray diffraction formed after 5 h: yield 116 mg (78%) Alternatively, diethyl ether can be layered on the THF solution after stirring, which results in immediate formation of fine white crystals: 120 mg (80% yield); elemental analysis (%) calcd for $C_{20}H_{24}F_6FeN_4O_6S_2$: C 36.93, H 3.72, F 17.53, N 8.61; found: C 37.19, H 3.96, F 17.35, N 8.61

2: A light yellow solution of L^8py_2 (41.1 mg, 0.139 mmol) and $[Fe(H_2O)_6](BF_4)_2$ (47.0 mg, 0.139 mmol) in CH_3OH (3 mL) was treated with NaO_2CPh (30.0 mg, 0.209 mmol). After stirring for 1 h, the yellow solution was treated with a solution of $NaBPh_4$ (95 mg, 0.28 mmol) in CH_3OH (2 mL), resulting in the immediate deposition of a bright yellow crystalline solid. The solid was collected by vacuum filtration, washed with CH_3OH and Et_2O, and dried under vacuum: 95 mg (86%). Crystals suitable for X-ray crystallography were grown from CH_3CN/Et_2O. Elemental analysis (%) calcd for $C_{49}H_{49}BFeN_4O_2$: C 74.25, H 6.23, N 7.07; found: C 74.69, H 6.11, N 7.21; UV/Vis (CH_3CN) λ_{max} (ε, $M^{-1}\,cm^{-1}$) 375 nm (450).

Crystal structure determination for **1**: Colorless plates from THF; $C_{20}H_{24}F_6FeN_4O_6S_2$, monoclinic, space group $P2_1/c$, $a = 11.352(2)$, $b = 14.333(3)$, $c = 16.013(3)$ Å, $\beta = 100.469(4)°$, $V = 2562.1(8)$ Å^3, $Z = 4$, $\rho_{calcd} = 1.686\,g\,cm^{-3}$, crystal dimensions: $0.36 \times 0.32 \times 0.08$ mm; diffractometer: Bruker CCD; $Mo_{K\alpha}$ radiation, 173(2) K; $2\theta_{max} = 50.1°$, 13032 reflections, 4540 independent ($R_{int} = 0.039$), direct methods; absorption correction semi-empirical from equivalents ($\mu = 0.840\,mm^{-1}$); Refinement (on F^2) with SHELXTL-Plus (version 5.10) and, 364 parameters, 75 restraints, $R_1 = 0.0421$ ($I > 2\sigma$) and wR_2 (all data) = 0.1094, Goof = 1.025, max/min residual electron density: 0.576/−0.602 e Å^{-3}.

Crystal structure determination for **2**: Yellow prisms from CH_3CN/Et_2O; $C_{51}H_{52}BFeN_5O_2$, monoclinic, space group $P2_1/c$, $a = 19.360(3)$, $b = 12.174(2)$, $c = 19.844(2)$ Å, $\beta = 112.64(1)°$, $V = 4316.6(11)$ Å^3, $Z = 4$, $\rho_{calcd} = 1.283\,g\,cm^{-3}$, crystal dimensions: $0.30 \times 0.25 \times 0.18$ mm; diffractometer: Bruker-Nonius MACH3S; $Mo_{K\alpha}$ radiation, 173(2) K; $2\theta_{max} = 51.96°$, 8446 reflections, 5092 independent ($R_{int} = 0.0391$), direct methods; no absorption correction required ($\mu = 0.396\,mm^{-1}$); Refinement (on F^2) with SHELXTL-Plus (version 5.10) and, 542 parameters, 0 restraints, $R_1 = 0.0661$ ($I > 2\sigma$) and wR_2 (all data) = 0.1317, Goof = 1.035, max/min residual electron density: 0.411/−0.463 e Å^{-3}.

CCDC 241381 and CCDC 241382 contain the supplementary crystallographic data for this paper. These data can be obtained free of charge via www.ccdc.cam.ac.uk/conts/retrieving.html (or from the Cambridge Crystallographic Data Centre, 12 Union Road, Cambridge CB2 1EZ, UK; fax: (+44) 1223-336-033; or deposit@ccdc.cam.ac.uk).

Received: August 3, 2004
Published online: December 15, 2004

Keywords: bioinorganic chemistry · coordination compounds · iron · peroxides · S ligands

[1] S. J. Lippard, J. M. Berg, *Principles of Bioinorganic Chemistry*, University Science Books, Mill Valley, **1994**.
[2] T. L. Poulos, B. C. Finzel, A. J. Howard, *J. Mol. Biol.* **1987**, *195*, 687.
[3] A. P. Yeh, Y. Hu, F. E. J. Jenney, M. W. W. Adams, D. C. Rees, *Biochemistry* **2000**, *39*, 2499.
[4] A. V. Coelho, P. Matias, V. Fülöp, A. Thompson, A. Gonzalez, M. A. Carrondo, *J. Biol. Inorg. Chem.* **1997**, *2*, 680.
[5] M. Sono, M. P. Roach, E. D. Coulter, J. H. Dawson, *Chem. Rev.* **1996**, *96*, 2841.
[6] R. Davydov, T. M. Makris, V. Kofman, D. E. Werst, S. G. Sligar, B. M. Hoffman, *J. Am. Chem. Soc.* **2001**, *123*, 1403.
[7] I. Schlichting, J. Berendzen, K. Chu, A. M. Stock, S. A. Maves, D. E. Benson, R. M. Sweet, D. Ringe, G. A. Petsko, S. G. Sligar, *Science* **2000**, *287*, 1615.
[8] D. L. Harris, G. H. Loew, *J. Am. Chem. Soc.* **1998**, *120*, 8941.
[9] J. A. Kovacs, *Chem. Rev.* **2004**, *104*, 825.
[10] C. Mathé, T. A. Mattioli, O. Horner, M. Lombard, J.-M. Latour, M. Fontecave, V. Nivière, *J. Am. Chem. Soc.* **2002**, *124*, 4966.
[11] M. D. Clay, F. E. Jenney, Jr., P. L. Hagedoorn, G. N. George, M. W. W. Adams, M. K. Johnson, *J. Am. Chem. Soc.* **2002**, *124*, 788.
[12] J. P. Emerson, E. D. Coulter, R. S. Phillips, D. M. Kurtz, Jr., *J. Biol. Chem.* **2003**, *278*, 39662.
[13] R. Silaghi-Dumitrescu, I. Silaghi-Dumitrescu, E. D. Coulter, D. M. Kurtz, Jr., *Inorg. Chem.* **2003**, *42*, 446.
[14] J. A. Halfen, H. L. Moore, D. C. Fox, *Inorg. Chem.* **2002**, *41*, 3935.
[15] J. Kaizer, M. Costas, L. Que, Jr., *Angew. Chem.* **2003**, *115*, 3799; Angew. *Chem. Int. Ed.* **2003**, *42*, 3671.
[16] Y. Zang, J. Kim, Y. Dong, E. C. Wilkinson, E. H. Appelman, L. Que, Jr., *J. Am. Chem. Soc.* **1997**, *119*, 4197.
[17] N. Lehnert, R. Y. N. Ho, L. Que, Jr., E. I. Solomon, *J. Am. Chem. Soc.* **2001**, *123*, 12802.
[18] N. Lehnert, R. Y. N. Ho, L. Que, Jr., E. I. Solomon, *J. Am. Chem. Soc.* **2001**, *123*, 8271.
[19] A. Mairata I Payeras, R. Y. N. Ho, M. Fujita, L. Que, Jr., *Chem. Eur. J.* **2004**, *10*, 4944.
[20] R. Y. N. Ho, G. Roelfes, B. L. Feringa, L. Que, Jr., *J. Am. Chem. Soc.* **1999**, *121*, 264.
[21] N. Lehnert, F. Neese, R. Y. N. Ho, L. Que, Jr., E. I. Solomon, *J. Am. Chem. Soc.* **2002**, *124*, 10810.
[22] J. Kim, Y. Zang, M. Costas, R. G. Harrison, E. C. Wilkinson, L. Que, Jr., *J. Biol. Inorg. Chem.* **2001**, *6*, 276.

